Research on the influence of hydrogen on mechanical properties of medium strength steels

Andrej Atrens, Qian Liu, The University of Queensland, St Lucia, Australia
Andrejs.Atrens@uq.edu.au

Summary

The linearly increasing stress test (LIST), together with cathodic hydrogen charging, was used to study the influence of hydrogen on martensitic steels. A methodology is described whereby the cathodic hydrogen charging is related to equivalent gaseous charging. For steels with yield strengths in the range 700-800 MPa, hydrogen had little influence at stresses below the yield stress. Hydrogen mediated fracture events, however, did contribute to the overall ductile fracture. Steels with yield strengths in the range 900 to 1400 MPa showed solid solution softening by hydrogen, and the fracture mode changed from ductile, cup-and-cone fracture to a macroscopically-brittle, shear fracture under the influence of hydrogen at slow applied stress rates.

1 Introduction

Hydrogen embrittlement (HE), an issue for high strength steels, has received much attention, including by our group [1,2,3,4,5,6,7,8,9,10,11,12,13,14,15,16,17,18,19,20, 21,22,23,24,25,26,27,28]. Section 2 outlines how electrolytic charging is related to the hydrogen fugacity in equivalent room temperature gas phase hydrogen charging. The key unknown is the Sievert's constant, which can be determined using thermal desorption spectroscopy (TDS) as outlined in Section 3. Sections 4 and 5 summarise research on steels with yield strengths (1) ~700 MPa and (ii) 900-1400 MPa.

2 Electrochemical H Charging

The equivalent hydrogen fugacity (pressure or activity) during cathodic charging is given by [1,2,3,4,29,30,31,32]:

$$f_{H_2} = A\exp\left(\frac{-\eta F}{\zeta RT}\right), \tag{1}$$

where F is the Faraday; R the gas constant; T the absolute temperature; A and ζ are constants related to the mechanism of the hydrogen evolution reaction (HER), as explained by Liu et al [3]; and the overpotential, η, is given by

$$\eta = E_c - E_H^0 \tag{2}$$

where E_H^0 is the hydrogen equilibrium potential, and E_c is the applied potential.

The corresponding hydrogen concentration, C_H, is given by

$$C_H = S\sqrt{f_{H_2}} \tag{3}$$

where S is the Sievert's constant.

C_H is measured in a permeability experiment and is given by [33]:

$$C_H = \frac{i_{\infty,\eta} L}{FD} \tag{4}$$

where i_∞ is the steady-state permeation current density for a particular charging condition, and L is the specimen thickness.

These equations indicate that:

$$i_\infty = \frac{FDS}{L}\left(f^e_{H_2}\right)^{1/2} = \frac{FDS}{L}\left(A\exp\left(-\frac{\eta F}{\zeta RT}\right)\right)^{1/2} \tag{5}$$

where $f^e_{H_2}$ is the fugacity during cathodic charging.

Thus permeability experiments can determine the critical parameters A and ζ. Fig. 1 presents an example.

Alternatively, permeability experiments can be carried out using hydrogen generated by free corrosion on the input side as might occur in service, and the hydrogen charging associated with these service conditions can be determined as shown by Liu et al [34].

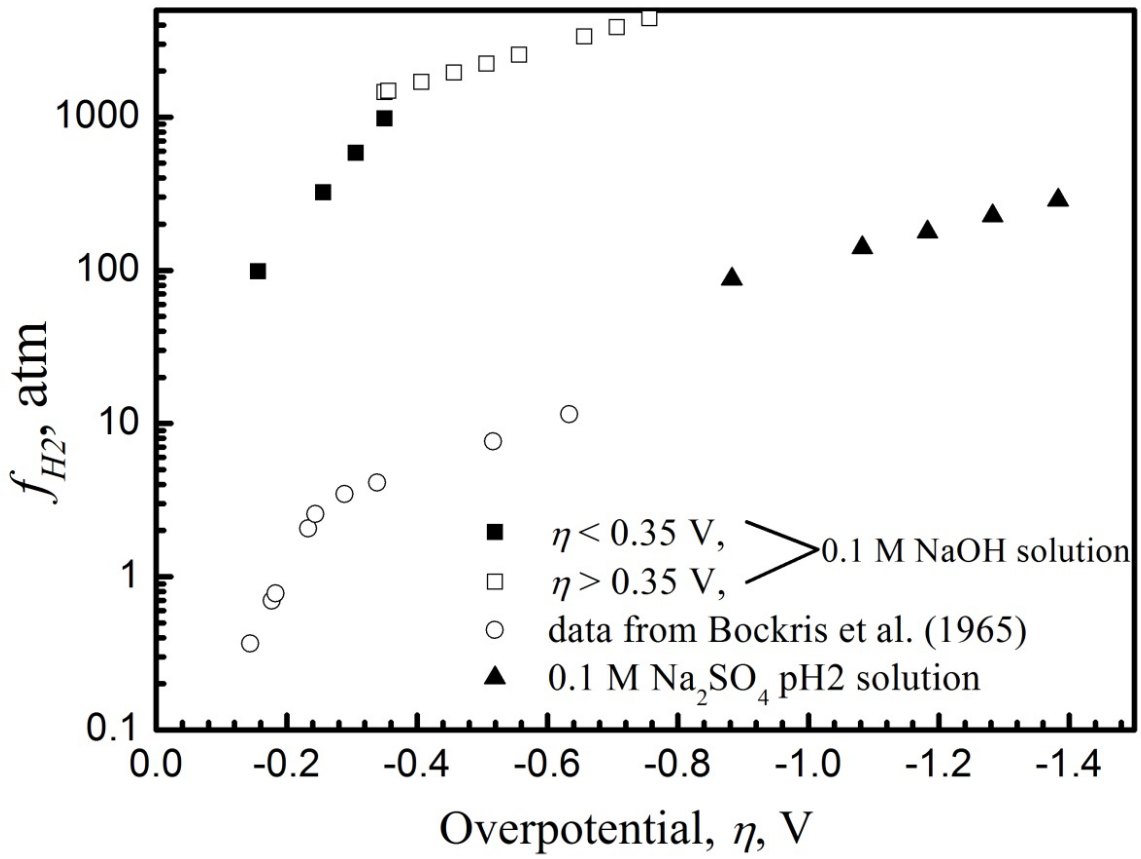

Fig. 1 Hydrogen fugacity, f_{H2}, versus overpotential, η (V), for the low interstitial steel [3] in (i) 0.1 M NaOH solution, and (ii) acidified pH 2 0.1 M Na_2SO_4 solution. The open circles were evaluated from

permeation data in 0.1 M NaOH from Bockris et al. [32].

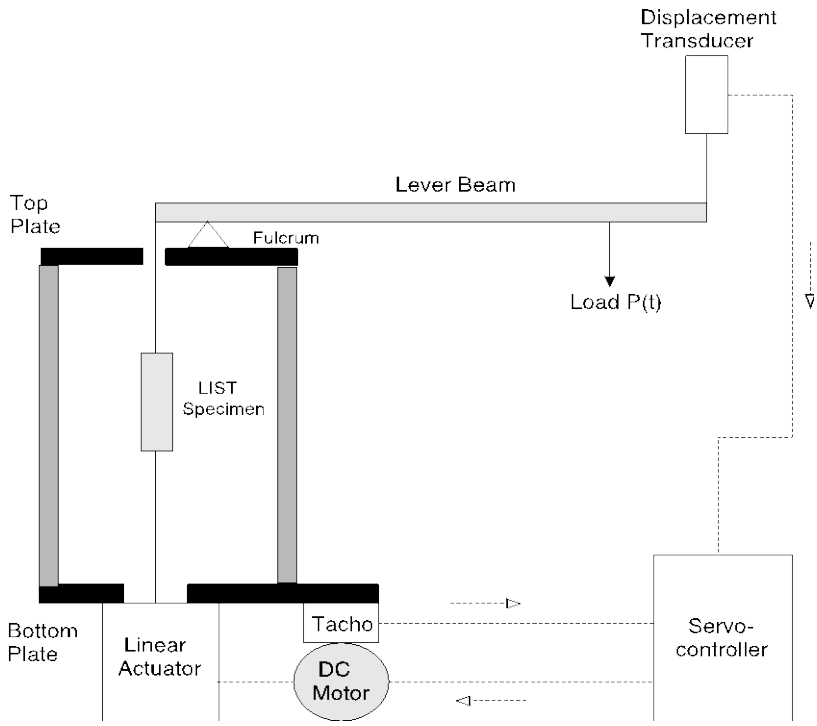

Fig. 2 Linearly increasing stress test (LIST) apparatus [23].

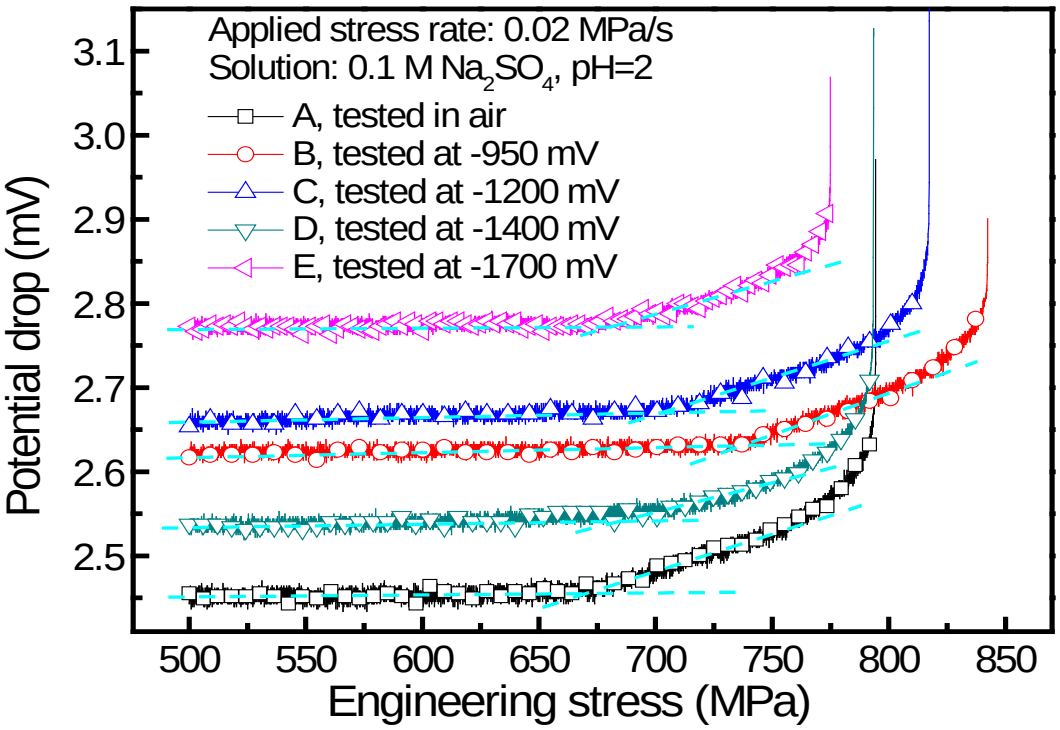

Fig. 3 Typical data for the determination of the yield stress or the threshold stress [1].

3 Thermal Desorption Spectroscopy

TDS can be used to determine *S* by measuring the hydrogen concentration after gas phase hydrogen charging at various pressures and fitting the data to Eq.(3).

4 LIST testing 3.5NiCrMoV: YS = 700-800 MPa

Fig. 2 illustrates the Linearly Increasing Stress Test (LIST) [23]. The specimen, on the left hand side of the fulcrum, is loaded at a steadily increasing rate by the steady motion of the weight on the right hand side driven from the equilibrium point by a synchronous motor. The specimen can be exposed to air or an environment. A potential drop allows identification of the yield stress or the threshold stress for the initiation of subcritical cracking by an environment [1,2]. The LIST is identical to the constant extension rate test (CERT) up to the onset of yielding or sub-critical crack growth. Thereafter the LIST is quicker as the specimen fractures at the maximum load (as in all load controlled test) whereas the CERT takes an additional time period for the specimen to extend [35]. The other advantage of the LIST is the ability to accurately measure the yield stress or the initiation stress.

For these quenched and tempered steels, subjected to LIST under cathodic charging conditions, Liu et al [1,2] found that (i) the steels had good resistance to hydrogen and failed by ductile overload, see Fig. 4, (ii) there was no hydrogen influence for stresses up to the yield stress, see Fig. 6, (iii) the influence of hydrogen was associated with localised plastic deformation and the final ductile fracture when the specimen was mechanically unstable, (iv) the hydrogen assisted fracture processes occurred during the final ductile fracture, and competed with that, see Fig. 5.

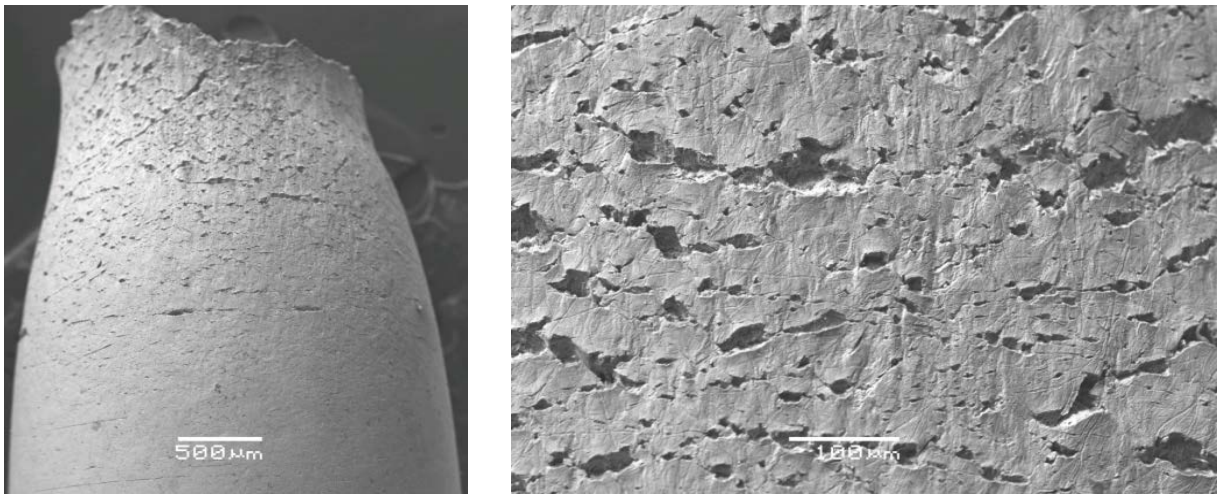

Fig. 4 Typical appearance of a 3.5NiCrMoV steel after LIST with hydrogen charging, showing significant necking, and secondary cracking only in the neck region, [1,2].

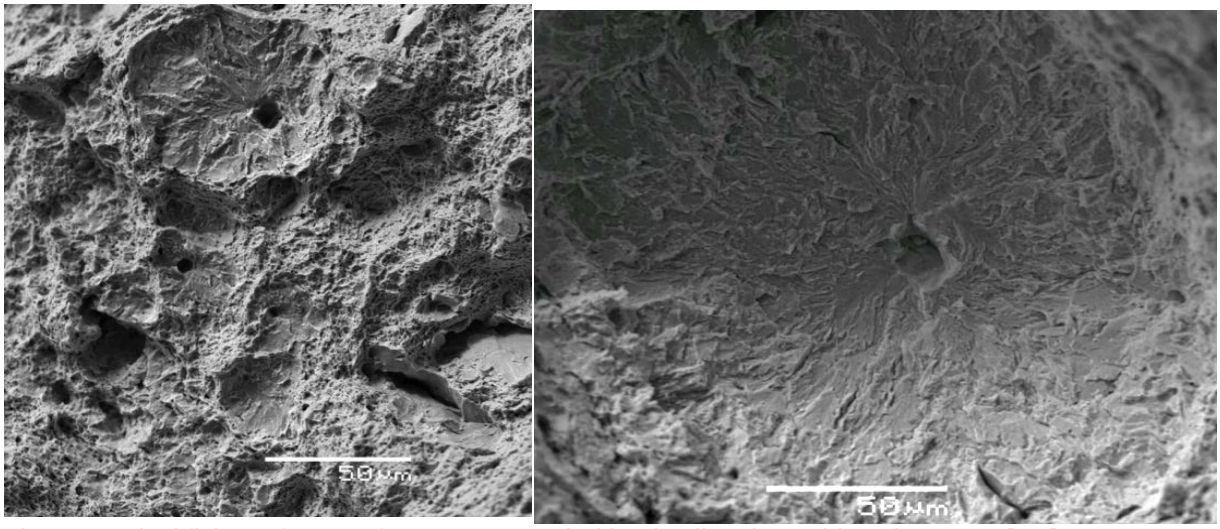

Fig. 5 A typical fisheye fracture feature surrounded by ductile microvoid coalescence [1,2].

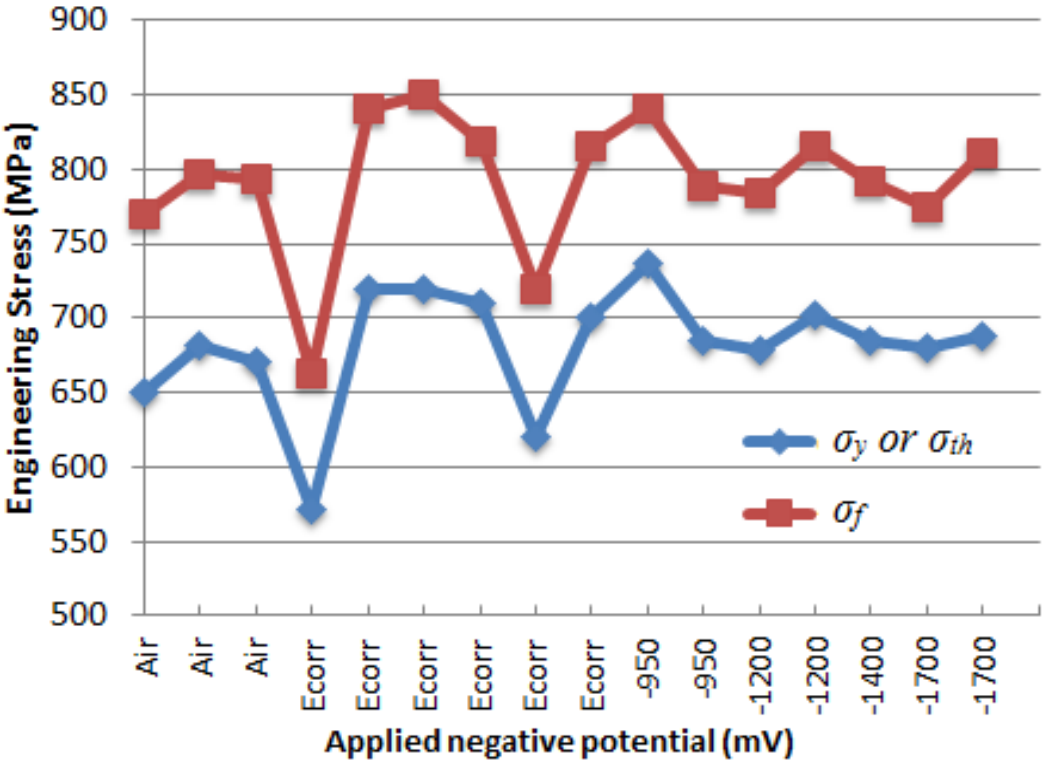

Fig. 6 The yield stress and fracture stress were largely unaffected by the cathodic hydrogen charging for the 3.5NiCrMoV, yield strength ~700 MPa, [1,2].

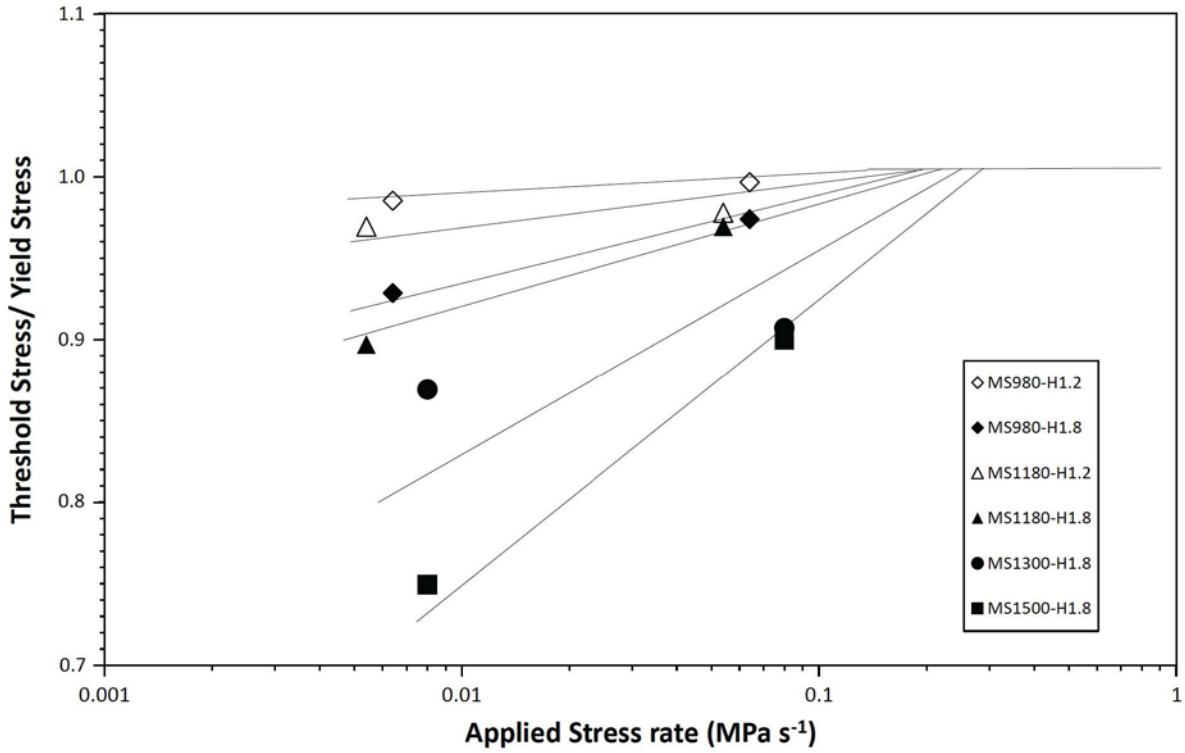

Fig. 7 Normalised yield strength for the four steels of increasing yield strength (900 - 1400 MPa) under mild (open symbols) and high hydrogen concentration, [36].

5 LIST testing MS-AHSS: YS = 900-1400 MPa

Four martensitic advanced high strength steels were studied [36] using LIST and cathodic hydrogen charging. The influence of hydrogen increased with the strength of the steel, increasingly negative cathodic charging potential producing higher hydrogen fugacities and with slower applied stress rates. The decease in the yield stress, see Fig. 7, was attributed to solid solution softening by hydrogen. With increasing hydrogen fugacity, the fracture mode changed from a ductile cup and cone fracture, to a macroscopically brittle shear fracture. Thus change in fracture mode caused by hydrogen is attributed to a dynamic interaction of hydrogen with dislocations during fracture in a mechanism that is envisaged to be somewhat similar to the hydrogen enhanced localised plasticity (HELP) mechanism of subcritical crack growth caused by hydrogen.

6 Conclusions

For the medium strength steels, with strengths in the range 700-800 MPa.

1. There was little influence of hydrogen at stresses below the yield stress.
2. There was an influence of hydrogen on the final fracture, when the specimen had become mechanically unstable. Then there was some contribution of hydrogen mediated fracture events to the overall ductile fracture.
3. A methodology was developed whereby the hydrogen charging conditions can be related to the equivalent gaseous charging conditions.

For steels with yield strengths in the range 900-1400 MPa.

1. These showed solid solution softening by hydrogen.
2. The fracture mode at the slow applied stress rates changed from ductile cup and cone fracture to a shear fracture under the influence of hydrogen

7 References

[1] Q Liu, B Irwanto, A Atrens, The influence of hydrogen on 3.5NiCrMoV steel studied using the linearly increasing stress test, Corrosion Science, 67 (2013) 193-203

[2] Q Liu, B Irwanto, A Atrens, The influence of hydrogen on the mechanical properties of some medium-strength Ni-Cr-Mo steels, Materials Science and Engineering A, 617 (2014) 200-210.

[3] Q Liu, AD Atrens, Z Shi, K Verbeken, A Atrens, Determination oft he hydrogen fugacity during electrolytic charging of steel, Corrosion Science, 87 (2014) 239-258.

[4] Q Liu, A Atrens, A critical review of the influence of hydrogen on the mechanical properties of medium strength steels, Corrosion Reviews, 31 (2013) 85-104.

[5] Q Liu, A Atrens, Reversible hydrogen trapping in a 3.5NiCrMoV medium strength steel, Corrosion Science 96 (2015) 112-120.

[6] W Dietzel, A Atrens, A Barnoush, Mechanics of modern test methods and quantitative-accelerated testing for hydrogen embrittlement, in Gaseous hydrogen embrittlement of materials in energy technoloigies RP Gangloff, BP Somerday eds, Woodhead, Vol 1, 2012, pp 237-273.

[7] D. Pérez Escobar, L. Duprez, A. Atrens, K. Verbeken, Influence of experimental parameters on thermal desorption spectroscopy measurements during evaluation of hydrogen trapping, Journal of Nuclear Materials 450 (2014) 32-41

[8] S Ramamurthy, A Atrens, Stress Corrosion Cracking of High Strength Steels, Corrosion Reviews, 31 (2013) 1-31.

[9] D Pérez Escobar, L Duprez, A Atrens, K Verbeken' Thermal desorption spectroscopy study of experimental Ti/S containing steels, Materials Science and Technology, 29 (2013) 261-267.

[10] D Pérez Escobar, E Wallaert, L Duprez, A Atrens, K Verbeken, Thermal desorption spectroscopy study of the interaction of hydrogen with TiC precipitates, *Metals and Materials International* 19 (2013) 741-748

[11] S Ramamurthy, WML Lau, A Atrens, Influence of applied stress rate on the stress corrosion cracking of 4340 and 3.5NiCrMoV steels under conditions of cathodic hydrogen charging, *Corrosion Science* 53 (2011) 2419-2429

[12] S Ramamurthy, A Atrens, The influence of applied stress rate on the stress corrosion cracking of 4340 and 3.5NiCrMoV steels in distilled water at 30 °C, Corrosion Science*,* 52 (2010) 1042–1051

[13] W Dietzel, PB Srinivasan, A Atrens, Testing and evaluation methods for stress corrosion cracking (SCC) in metals, Chapter 3 in *Stress corrosion cracking: theory and practice*, Edited by V.S. Raja, T. Shoji, Woodhead Cambridge, (2011) 133-166

[14] W. Dietzel, A. Atrens, A. Barnoush, Mechanics of modern test methods and quantitative-accelerated testing for hydrogen embrittlement, in *Gaseous hydrogen embrittlement of materials in energy technologies*, edited by R.P. Gangloff, B.P. Somerday, Woodhead, (2011) pp 237-273

[15] E Villalba, A Atrens, Metallurgical Aspects Of Rock Bolt Stress Corrosion Cracking, *Materials Science and Engineering A*, 491 (2008) 8-18

[16] E Villalba, A Atrens, SCC of Commercial Steels Exposed to High Hydrogen Fugacity, *Engineering Failure Analysis,* 15 (2008) 617-641

[17] E Gamboa, A Atrens, Material influence on the stress corrosion cracking of rock bolts, *Engineering Failure Analysis,* 12 (2005) 201-225

[18] E Gamboa, A Atrens, Environmental Influence on the Stress Corrosion Cracking of Rock Bolts, *Engineering Failure Analysis* 10 (2003) 521-558

[19] E Gamboa, A Atrens, Stress Corrosion cracking fracture mechanisms in rock bolts, *Journal of Materials Science* 38 (2003) 3813-3829

[20] NN Kinaev, DR Cousens, A Atrens, The Crack Tip Strain Field of AISI 4340 Part III Hydrogen Influence, *J Materials Science* 34 (1999) 4931-4936

[21] A Atrens, ZF Wang, ESEM observations of SCC initiation for 4340 high strength steel in distilled water, *J Materials Science* 33 (1998) 405-415

[22] A Oehlert, A Atrens, SCC Propagation in Aermet 100, *J Materials Science* 33 (1998) 775-781.

[23] A Atrens, CC Brosnan, S Ramamurthy, A Oehlert, IO Smith. Linearly Increasing Stress Test (LIST) for SCC Research, *Measurement Science and Technology*, 4 (1993) 1281-1292

[24] S Ramamurthy, A Atrens. The Stress Corrosion Cracking of As-Quenched 4340 and 3.5NiCrMoV Steels Under Stress Rate Control in Distilled Water at 90C, *Corrosion Science,* 34 (1993) 1385-1402

[25] ZF Wang, A Atrens. Initiation of Stress Corrosion Cracking for Pipeline Steels in a Carbonate-Bicarbonate Solution, *Metallurgical and Materials Transactions*, 27A (1996) 2686-2691

[26] A Atrens, NF Fiore, K Miura, Dislocation damping and hydrogen pinning in austenitic stainless steels, Journal of Applied Physics, 48 (1977) 4247-4251.

[27] A Atrens, Service performance of engineering materials, Journal of Materials Science and Technology 21 (2005) 81-85.

[28] E Gamboa, A Atrens, Relationship of laboratory tests of rock bolt SCC to service failures of rock bolts, Hydrogen effects on material behaviour and corrosion deformation interactions, NR Moody, AW Thompson, RE Ricker eds, TMS, (2003) 647-661.

[29] A. Atrens, D. Mezzanotte, N.F. Fiore, M.A. Genshaw, Electrochemical studies of hydrogen diffusion and permeability in Ni, Corrosion Science 20 (1980) 673-684

[30] J.O.M. Bockris, J. McBreen, L. Nanis, The Hydrogen Evolution Kinetics and Hydrogen Entry into a-Iron, Journal of The Electrochemical Society 112 (1965) 1025-1031.

[31] J. Bockris, A. Reddy. Modern Electrochemistry, 1970, Plenum Press, New York

[32] J.O.M. Bockris, P.K. Subramanyan, The equivalent pressure of molecular hydrogen in cavities within metals in terms of the overpotential developed during the evolution of hydrogen, Electrochimica Acta 16 (1971) 2169-2179

[33] U. Hadam, T. Zakroczymski, Absorption of hydrogen in tensile strained iron and high-carbon steel studied by electrochemical permeation and desorption techniques, International Journal of Hydrogen Energy 34 (2009) 2449-2459

[34] Q. Liu, J. Venezuela, M. Zhang, Q. Zhou, A. Atrens, Study on hydrogen permeation in DP and Q&P grades of AHSS under cathodic charging and service conditions, Baosteel Conf (2015).

[35] N Winzer, A Atrens, W Dietzel, G Song, KU Kainer, Comparison of the Linearly Increasing Stress Test and the Constant Extension Rate Test in the Evaluation of Transgranular Stress Corrosion Cracking of Magnesium, *Materials Science and Engineering A*, 472 (2008) 97-106.

[36] J Venezuela, Q Liu, M Zhang, Q Zhou, A Atrens, The influence of hydrogen on the mechanical and fracture properties of some martensitic advanced high strength steels studied using the linearly increasing stress test, Corrosion Science accepted for publication 26 June 2015.